State Key Laboratory for Diagnosis and Treatment of Infectious Diseases[1], The First Affiliated Hospital of Medical College; Institute of Pharmacology & Toxicology[2], College of Pharmaceutical Sciences, Zhejiang University, Hangzhou, China

Correlation of pharmacokinetic features and tissue distribution with toxicity of Q39, a hypoxic cell cytotoxic agent

Difeng Zhu[1,2], Jianshu Lou[2], Honghai Wu[2], Peihua Luo[2], Lanjuan Li[1]

Received March 9, 2010, accepted March 24, 2010

Dr. Peihua Luo, Institute of Pharmacology and Toxicology, School of Pharmaceutical Sciences, Zhejiang University, 388# Yuhangtang Rd., Hangzhou, Zhejiang 310058, China
peihualuo@zju.edu.cn
Dr. Lanjuan Li, State Key Laboratory for Diagnosis and Treatment of Infectious Diseases, The First Affiliated Hospital of Medical College, Zhejiang University, Zhejiang 310058, China

Pharmazie 65: 683–689 (2010) *doi: 10.1691/ph.2010.0064*

3-(4-Bromophenyl)-2-(ethylsulfonyl)-6-methyl- quinoxaline 1,4-dioxide (Q39), is one of synthesized tirapazamine (TPZ) analogues that has been investigated preclinically as a hypoxic anticancer candidate. To date, there has not been a study to systematically evaluate the toxicity and pharmacokinetics of Q39. In the present study, we characterized the toxicity profile of Q39 in ICR mice. No toxicities were observed in mice treated with Q39 at dose levels that 168 mg/kg. LD_{50} value was 257.8 mg/kg (95% confidence interval = 231.1-287.5 mg/kg), which was 3.3-fold higher than that of TPZ. For the plasma pharmacokinetic assessment, a balb/c nude mice bearing K562 leukemia cell xenografted model was introduced and dosed with Q39 intravenous (*i.v.*)(1.0 mg/kg). Rapid resolution liquid chromatography coupled with tanderm mass spectrometry quantitative detection method (RRLC-MS/MS) was used to quantitatively determine plasma concentration. The RRLC-MS/MS method was validated within the concentration range 25-2000 ng/mL, and the calibration curves were linear with correlation coefficients of >0.999. Following intravenous administration to nude mice (1.0 mg/kg), plasma concentrations declined rapidly from 1063.3 μg/mL at 10 min to 81.5 μg/mL at 3 h. Elimination was triexponential, with $T_{1/2}$ values of 1.4 h. The *CL* was 930.0 mL/h/kg, the V_d was 1.88 L/kg, and the $AUC_{0-\infty}$ was 1080.5 ng/mL h. In the tissue distribution assay, concentration of Q39 was higher in the heart, liver, spleen and tumor tissues. The present study offers insights into the toxicological and pharmacologic profiles of Q39 which could help to optimize the dosage of Q39 for the future research and development.

1. Introduction

It is widely accepted that the inefficient microvascular system in solid tumors limits the delivery of some anticancer drugs to their target cells, and that gives rise to a wide distribution of oxygen concentrations, with more severely hypoxic regions than found in most normal tissues (Ahlskog et al. 2009; Svensson et al. 2008). Tumor-associated hypoxia contributes to tumor progression, and can affect cure rates in both radiotherapy and chemotherapy (Selvendiran et al. 2009; Rockwell et al. 2009; Yang et al. 2003). The widespread occurrence of hypoxia in tumors presents an opportunity to develop tumor-selective prodrugs that are metabolized to cytotoxic products via bioreductive processes that are inhibited by oxygen (Tredan et al. 2009; Jiang et al. 2007). As a result, this is meaningful in the development of drugs that are activated by enzymatic reduction (bioreductive drugs) under hypoxic conditions.

Tirapazamine (TPZ), a benzotriazin 1,4-dioxide (BTO), has been reported as one of the most potent anti-tumor compounds in hypoxia, because of its simple structure and strong hypoxic

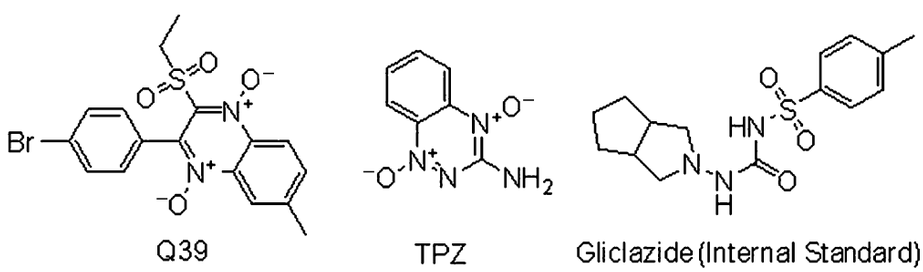

cytotoxicity against a variety of human cancer cells (Marcu et al. 2006; Reddy et al. 2009). Despite the very promising results obtained in various preclinical studies and early-phase clinical trials, several Phase III trials have failed to demonstrate any survival benefit of adding TPZ to chemotherapy or radiation therapy in non-small cell lung cancer or head and neck cancer (Yang et al. 2005). TPZ has shown promising clinical activity, although at the cost of significant toxicity (including neutropenia, thrombocytopenia, diarrhea, nausea, vomiting, cramping, and fatigue) (Zhang et al. 2007). While there is every prospect that TPZ will prove to be useful in cancer treatment, its selectivity against hypoxic cells in tumors is lower than the differential between anoxic and oxic (20% O2) cells in culture (Yang et al. 2005). This may reflect the smaller range of oxygen tensions *in vivo*, but might also result from a failure of TPZ to reach the most hypoxic cells in tumors. In support of this, Durand and Olive have shown that the activity of TPZ against cells in the center of V79-171b multicellular spheroids is diminished when the whole spheroid is made hypoxic and have suggested that rapid metabolic consumption of TPZ might limit its activity against hypoxic cells in tumors. These studies raise the question as to whether analogues of TPZ with greater metabolic stability might be preferable, but the inference that extravascular diffusion of TPZ is a limiting factor is currently based on quite indirect evidence. In addition, new analogues with higher solubility (or potency) than TPZ would be of distinct advantage.

TPZ has a number of limitations which makes the exploration and development of novel analogues a potentially fruitful endeavor. Q39, as an 1,4-dioxide analogue of TPZ, has been demonstrated in a previous study to induce apoptosis in cancer cells and exhibit great anticancer activity against K562 cells in hypoxic environment (Weng et al. 2007). Additionally, we investigated the impact of Q39 on the MAPK signaling pathways, and showed that Q39 treatment significantly decreased p-ERK and increased p-JNK, indicating that Q39 may influence MAPK family to block HIF-1α protein synthesis, and finally decrease HIF-1α level. Importantly, we also found that Q39 exhibited *in vitro* antiproliferative activity on all tested cell lines in a dose-dependent manner, and the IC_{50} values of Q39 for the five tumor cell lines were below 10.0 μM in hypoxia and in normoxia (Weng et al. 2007).

It is essential to determine the toxicity profiles of compounds early in the drug discovery stage to facilitate the subsequent research and development. The pharmacokinetic and tissue distribution information for Q39 is important in determining its therapeutic activity and helps to decide the frequency of dosing. The goal of the present study is to characterize the murine toxicology, pharmacokinetics and tissue distribution of Q39 in nude mice bearing K562 human leukemia cell xenografts.

2. Investigations and results

2.1. Toxicological evaluations

Six different doses (168, 198, 233, 275, 323, and 380 mg/kg) were examined for Q39 with each dosage group consisting of ten mice, and drug-related clinical signs of mortality, activity loss, astasia, hyperspasmia, and loss of body weight are illustrated in Table 1. Toxic events were scored on the basis of severity with 1–3 being mildly severe, 4–6 being moderately severe and above 6 as being very severe. A total score was the computed based on the occurrence of individual toxic events at each dose, with a higher score corresponding to higher toxicity. Low dosage group (168 mg/kg) did not exhibit any toxic or deleterious effects. In the various dosage groups, if one mouse exhibited activity loss, astasia, or hyperspasmia the others were observed to do the same. The greatest severity of activity loss, astasia, and hyperspasmia was seen in the highest dose treated mice. Mortality was also seen in this group resulting in the death at 380 mg/kg. A maximal decrease in body weight was observed from the two to six days following *i.v.* administration, after which, in surviving mice, recovery started.

Table 1: Effects of Q39 on clinical signs at termination of study

Compound	Dose level (mg/kg)	Mean score for clinical signs					Total score
		Mortality	Activity loss	Astasia	Hyperspasmia	Weight loss [a]	
Vehicle	0	0	0	0	0	0	0
Q39	168	0	0	0	0	0	0
	198	1	1	0	0	1	3
	233	2	1	1	0	2	6
	275	3	2	2	1	2	10
	323	4	3	3	2	3	15
	380	4	4	4	3	4	19

[a] Mean body weight change was scored following i.v. administration, after which, in surviving mice, recovery started

The results of the i.v. toxicity evaluations, expressed as LD_{50} values estimated 14 days after the first injection, are presented in Table 2. The studies on acute toxicology showed that in the case of administration of Q39 in mice, LD_{50} was 257.8 mg/kg (95% confidence interval: 231.1–287.5 mg/kg) for intravenous injection. The relative LD_{50} was 3.3-fold higher based on population-based data compared with reports from the literature (Dorie et al. 1997).

In accordance with the above results, it was demonstrated that Q39 exhibited lower toxicity and relatively higher safety as compared with TPZ.

2.2. Pharmacokinetic studies

The method developed was successfully used to analyze Q39 in nude mice plasma. It was sensitive enough to permit quantitation of Q39 in plasma with acceptable accuracy and precision over a period of 6 h. The levels of Q39 in the plasma were measured to be maximal at the earliest time points tested. Following bolus intravenous administration of Q39 (1.0 mg/kg) to nude mice, plasma concentrations declined rapidly from 1063.3 mg/ml at

Table 2: LD_{50} and 95% confidence interval (CI) of intravenous injection of Q39 in mice (Bliss Method)

Dose (mg/kg)	Log dose	Number of animals	Number of dead animals	Death rate (%)	Probability units (Y)	LD_{50} and 95% CI (mg/kg)
168	2.2253	10	0	0	3.04	
198	2.2967	10	1	10	3.72	
233	2.3674	10	3	30	4.48	257.8
275	2.4393	10	4	40	4.75	(231.1–287.5)
323	2.5092	10	8	80	5.84	
380	2.5798	10	10	100	6.96	

Abbreviations used, LD_{50} half lethal dose, CI confidence interval

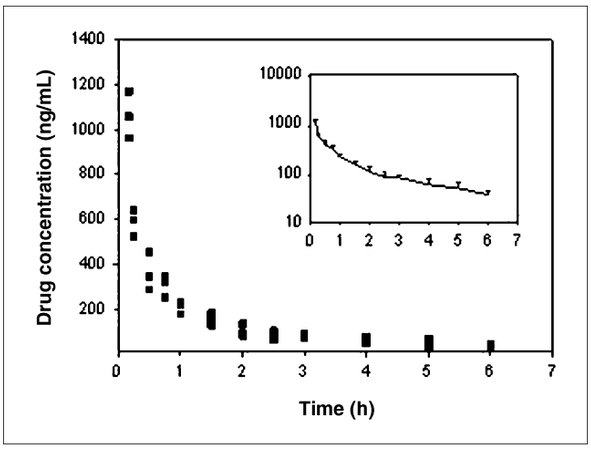

Fig. 1: Plasma pharmacokinetics of Q39 following intravenous administration to nude mice at a dose of 1.0 mg/kg. There were three nude mice for each time point. The insert curves show the mean with semi-logarithmic representation (data points show the mean ± s.d.)

Table 3: Pharmacokinetic parameters for Q39 in nude mice dosed by intravenous injection

Pharmacokinetic parameters	Unit	Value[a]	
		Mean	SD
K_{iv}	h^{-1}	0.50	0.04
$T_{1/2}$	H	1.40	0.12
$AUC_{0\text{-}t}$	ng/mL × h	1004.81	84.48
$AUC_{0\text{-}\infty}$	ng/mL × h	1080.54	92.67
CL	mL/h/kg	930.00	84.00
Vd	L/kg	1.88	0.12
Cmax	ng/mL	1063.33	103.54
MRT	H	1.32	0.10

[a] Data were analyzed by a non-compartmental approach

10 min to 83.5 mg/ml at 2.5 h. The plasma concentration-time profile of Q39 after intravenous administration is illustrated in Fig. 1. At 4 h after dosing, the concentration was less than 60 mg/ml. Regression analysis indicated that plasma concentrations of Q39 declined triexponentially. Data were analyzed according to a non-compartmental analysis using DAS 2.0 and the relevant pharmacokinetic parameters were computed (Table 3). These data validated a relatively rapid elimination from the blood compartment with e.g. an elimination rate constant (K_{iv}) of $0.50 \pm 0.04\,h^{-1}$ and a biological half-life ($T_{1/2}$) of 1.40 ± 0.12 h. The biological half-life of TPZ has previously been described in mice models which was 0.59 ± 0.01 h (Graham et al. 1997). Comparable pharmacokinetic analyses in patients have determined the half-life ($T_{1/2}$) of TPZ as 0.68 ± 0.07 h (Aquino et al. 2004). These results indicated that the clearance of Q39 was slower than that of TPZ. The volume of distribution of Q39 (1.88 ± 0.12 L/kg, Table 3) corresponds to an extra-vascular distribution and suggested that some tissues (organs) preferentially retain Q39 than the others (i.e., the volume is 20-fold larger than the blood volume of a mouse (60–80 mL/kg)).

2.3. Tissue distribution of Q39

In order to elucidate the bio-distribution in the tissues, the concentration of Q39 after intravenous administration to nude mice bearing K562 human leukemia cell xenografts was determined in the plasma, tumor, and organs (kidneys, liver, heart, lung, spleen, brain). Four different post-administration time points (30, 90, 180, and 360 min) were chosen to examine the tissue distribution of Q39. The bio-distribution of Q39 after single administration is shown in Fig. 2. Following intravenous injection, all the studied tissues show an accumulation of Q39 in the tissues such as liver, spleen, heart and tumor, which accumulate higher levels of Q39 than the other tissues like kidneys, lung and brain. At 6 h, the concentrations of Q39 were 86.33 ± 34.53 ng/g (heart), 58.00 ± 12.12 ng/g (liver), 85.67 ± 74.07 ng/g (spleen), 32.67 ± 20.23 ng/g (lung), 45.67 ± 31.18 ng/g (kidney), 43.33 ± 27.47 ng/g (brain), and 265.67 ± 228.50 ng/g (tumor), indicating a highly selective localization in the xenografts by the Q39.

The amounts of Q39 localized in K562 xenografts (ID%/g tissue) surpassed those in most normal organs at 3 h post-injection and were approaching those in the spleen and heart (Fig. 3a). It is noteworthy that Q39 was cleared at a much slower rate from the xenografts than from the normal organs (Fig. 3a), and at 3 h post-injection the T/NT tissue localization ratio reached 1.67 and 1.33 for the heart and the spleen, respectively (Fig. 5b). At 6 h, the T/NT ratios were 3.08 (heart), 4.58 (liver), 3.10 (spleen), 8.13 (lung), 5.82 (kidney) and 6.13 (brain), respectively, indicating a highly selective localization in the xenografts by the Q39.

3. Discussion

Anticancer therapy needs to be improved with new molecules that present higher effectiveness and a more favorable safety profile. One of the reasons that TPZ failed in phase III clinical trail, is due to significant toxicities associated with the clinical use of TPZ that preclude its administration at doses high enough to fully exploit tumor hypoxia throughout a treatment regimen. Aditionally, rapid metabolic consumption limited its activity against hypoxic cells in tumors. Thus, it is a great challenge for researchers to explore novel hypoxia-selected compounds. The novel antitumor compound Q39 may be clinically useful as a potential anticancer agent. Although it is difficult to extrapolate preclinical pharmacological results to clinical situations, characterization of toxicology, pharmacokinetics, and bio-distribution of Q39 in mice may facilitate its preclinical investigation and clinical research.

Traditionally, in toxicological studies, the relationship between the probability of acute lethal toxicity and treatment-related parameters is predictable by rating scale. Dose intensity is closely related to the probability and severity of acute toxicity, which is a typical observation for hierarchical, early-reacting signs (Zhu et al. 2009). Cytotoxicity assay demonstrated that Q39 is a potential and highly efficient anti-cancer compound in tested cell lines with IC_{50} values of 0.18–8.88 μM in hypoxia and 0.33–8.74 μM in normoxia (Weng et al. 2007). In the present study, toxicology of Q39 given 14 days in mice was determined to provide additional pre-clinical animal data. The primary objective was to determine acute toxicity by drug-related clinical signs of activity loss, astasia, hyperspasmia, and loss of body weight. The 380 mg/kg group had the highest toxicity scores and displayed comparable toxicity or deleterious effects for each clinical observation, including mortality. In the toxicity study, it was found that Q39 had a LD_{50} of 257.8 mg/kg (95% CI: 231.1–287.5 mg/kg). Interestingly, Q39 displayed lower toxicity than its parent compound TPZ. It should be noted that we have shown in recent antitumor studies in mice models that up to 168 mg/kg of Q39 was not toxic. In contrast, TPZ, a bioreductive drug with selective toxicity for hypoxic cells in tumors was found to have a LD_{50} of 0.44 mM/kg (78.4 mg/kg) (Yang et al. 2005) which was higher than that of Q39.

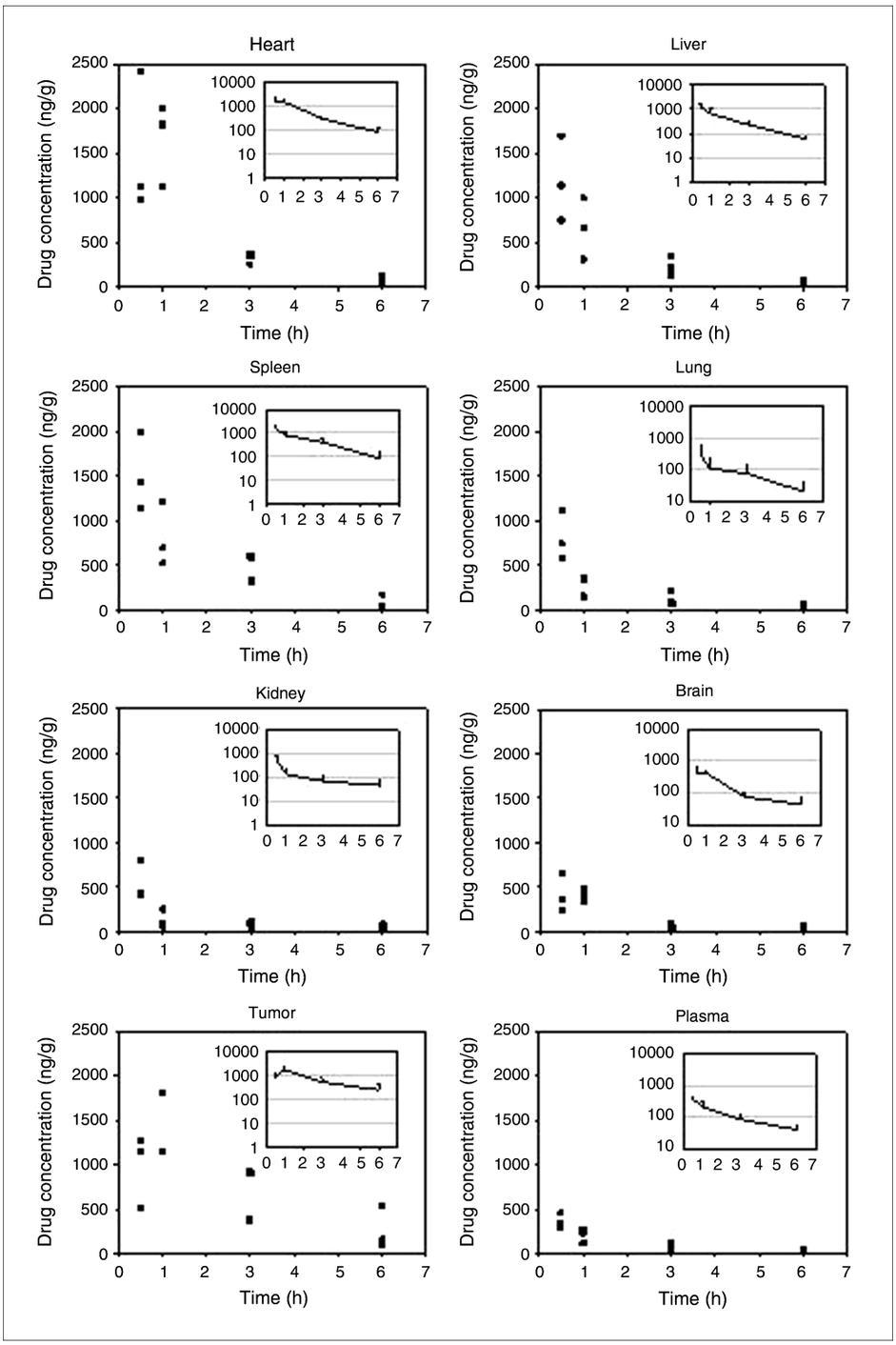

Fig. 2: Q39 concentrations in plasma and tissues (heart, liver, spleen, lung, kidney, brain, tumor) in nude mice bearing K562 human leukemia cell xenografts after intravenous injection with 1.0 mg/kg. Q39 concentrations for each organ are represented in ng/g tissue for each animal. The insert curves show the mean with semi-logarithmic representation (*Error bars* represent SD, n = 3)

The initial design of this study called for an analysis of plasma samples or tissues for Q39 by HPLC with UV detection as previously used (Chavanpatil et al. 2006). However, the limit of quantification (LOQ) in plasma was found to be approximately 400 ng/mL. In order to determine if the LOQ would be sufficient to generate a fully defined plasma concentration-time profile for Q39, a simulated kinetic model based on our preliminary experiment data was created and evaluated. The results of this model indicated that a LOQ of 32 ng/mL would be required to complete the PK arm of this study. As a result of this simulated kinetic modeling, a new method using HPLC coupled with tandem mass spectrometry (MS/MS) as the detection mode was developed and validated for this study. The RRLC-MS/MS method has a LOQ range of 25–2000 ng/mL and our results on fully defining the terminal linear phase of Q39 (Fig. 1) demonstrated that this more sensitive methodology was necessary. This simple and accurate analytical RRLC-MS/MS method was employed for the determination of Q39 in nude mice plasma. The method was

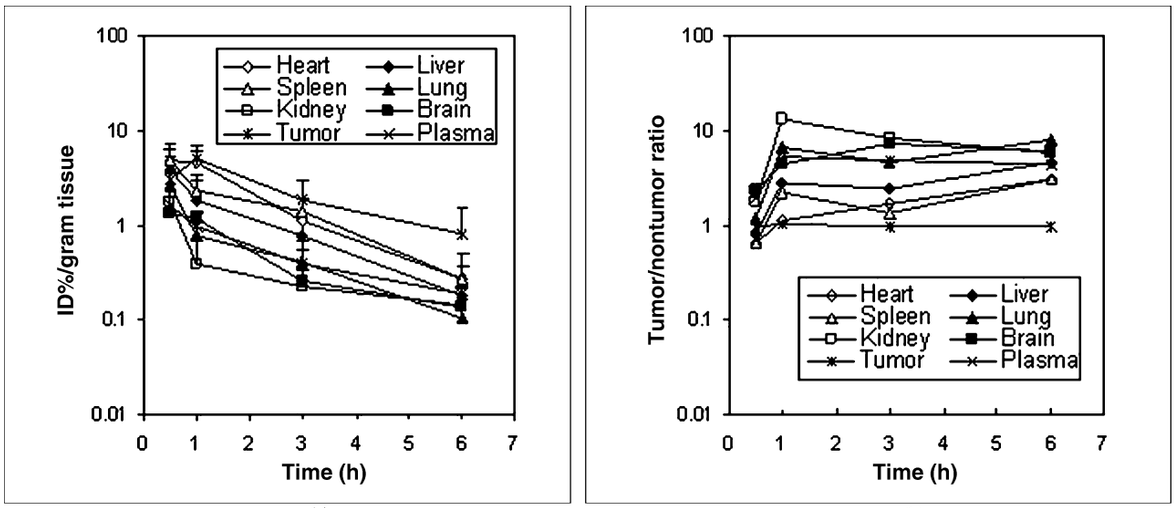

Fig. 3: Q39 localizes selectively in K562 xenografts in nude mice. K562 tumor-bearing mice were injected intravenously with Q39 and killed at predefined intervals. The xenografts, along with normal mouse organs, were collected, weighted, and determined concentrations localized in the tissues. Distribution of the Q39 in K562 tumor-bearing mice at various time points post-administration expressed as ID%/g tissue (a) or T/NT ratio (b). Data in (a) represents mean (±SD), obtained from three mice sampled at each time point, and in (b) is the means from the same three mice

further applied to investigate the tissue distribution and evaluate the pharmacokinetics of Q39 after intravenous administration to nude mice.

As stated previously, evaluations of pharmacokinetics of Q39 can be important in the selection of an appropriate dose and schedule of administration to achieve effective plasma concentrations of the test compound. Optimization of a dosing regimen can be achieved by characterization of the pharmacokinetic properties of an agent. The present work is the fist report of *in vivo* pharmacokinetics parameters of Q39 in an animal model, i.e., the nude mouse model. Intravenous administration was performed and the $AUC_{0\text{-}\infty}$ value was calculated. The plasma concentration time curves were analyzed using non-compartmental modeling for Q39 as described in the "Statistical analysis" section. Q39 has typical plasma concentration-time curves for intravenous administration. The pharmacokinetic parameters of Q39 were compared to other hypoxia-activated prodrugs BTOs (Hay et al. 2007), tirapazamine (TPZ) (Robin et al. 1995), banoxantrone (formerly AQ4N) (Steward et al. 2007), PR-104 (Hicks et al. 2007), and NLCQ-1 (Reid et al. 2003). The pharmacokinetic comparison of these compounds indicates that after i.v. administration, elimination half-life of Q39 (1.4 h), was much longer than that of tirapazamine (0.68 h), PR-104 (1.1 h), NLCQ-1 (0.68 h). MRT, which better describes the drug's time course, was 1.32 h for intravenous administration. It seems that C_{max} was not possible to calculate due to its fast concentration decrease in plasma levels. The levels of Q39 remained above the limit of quantification up to 6 h after intravenous administration. Results suggest that Q39 presents improved features compared to other hypoxia-activated prodrugs.

Using the sensitive RRLC-MS/MS methodology, we could accurately measure tissue concentrations of Q39. Following intravenous injection administration, Q39 tissue levels (Fig. 2) were still detected up to 6 h in all the studied tissues. The highest concentrations of Q39 were found in the tumor, which suggests that this novel drug could be eliminated via this organ. The second highest concentration was found in heart tissue, followed by spleen, liver, kidney, brain, plasma and lung. Once Q39 has penetrated the brain and the tumor, it does not enter an elimination phase, as the log linear portion of the log concentration *versus* time plot remains almost constant or increasing from 0.5–1 h (Fig. 2). Q39 was rapidly eliminated from all studied tissues and accumulated in the tumor at relevant levels, which could reach 5.2% of the injected dose per gram of tumor tissue, 1 h after intravenous injection. Relatively high drug levels were found in the spleen and the heart, in contrast to the lung, kidney, brain and plasma, where relatively low levels were measured. The highest levels of Q39 that we found in tumor tissue would imply that Q39 might be a better candidate for treatment of leukemia, since this prodrug specifically accumulates in tumor tissue.

In summary, the results provide a basis for further evaluation of Q39 as a new chemotherapeutic agent. The present study shows that Q39 and TPZ have different pharmacokinetic profiles when administered as single intravenous doses to mice. Q39 accumulated in heart, liver and spleen, and resided in the tumor for an extended time. Although Q39 is an interesting candidate for therapeutic use, due to its potential characteristics to specifically target leukemia, the slow elimination of the compound might make it challenging to design appropriate dosage regimes. Future studies are needed to determine if the tumor retention of Q39 is related to the sensitivity of the xenograft tumor and if the tumor retention of Q39 occurs in patients with solid tumors and how the tumor disposition of Q39 impacts antitumor response in patients with solid tumors.

4. Experimental

4.1. Chemicals and reagents

Q39 was synthesized in the ZJU-ENS Joint Laboratory of Medicinal Chemistry (Zhejiang, China). The structures of Q39 were determined by IR, MS, and NMR. Column chromatography was carried out with silica gel 60 Merck for purification, and the purity of Q39 was >99%. Gliclazide as internal standard (IS) was obtained from National Institute for the Control of Pharmaceutical and Biological Products of China (Beijing, China). Ammonium formate was purchased from Sinopharm Chemical Reagent Co. (Shanghai, China). Ultrapure water was obtained from a Milli-Q$^{\circ,R}$ Plus apparatus (18.2 MΩ cm, Millipore, MA, USA). Other chemicals were all of analytical grade.

4.2. Animals and study groups

Five to six week-old male and female ICR mice (20–24 g) were obtained from the Zhejiang University Laboratory Animal Centre (Zhejiang, China), and handled in accordance with the Guide for the Care and Use of Laboratory Animal. Nude mice (5–6 weeks old) were obtained from SLAC Laboratory Animal CO. (Shanghai, China). All animals were maintained in an ammonia-free environment in a defined and pathogen-free colony. Animals were quarantined for approximately 1 week prior to their use for

toxicology study, tumor propagation or pharmacokinetic testing. They were given food and water *ad libitum*. For the toxicology study, a total of 60 male and female ICR mice were randomly assigned to one of six Q39 dose groups (168, 198, 233, 275, 323, 380 mg/kg) with an equal number of males and females in each of the six groups. These mice were used for a 14 day toxicity study in which the mice were given different doses of Q39. For the pharmacokinetic study, K562 cells were inoculated subcutaneously in either of the hind legs of each mouse (5×10^6 cells/each) to establish a human-nude mice leukemia xenograft model, as described previously (Fang et al. 2007). Tumors were then allowed to grow to the pre-determined size range (usually between 100–200 mg, tumors outside the range were excluded). A total of 39 nude mice were randomly assigned to receive a single 1.0 mg/kg dose intravenous of Q39 formulated in 0.9% sodium chloride, and blood was collected at different time points ranging from 10 min to 12 h after drug administration (n = 3 per time points). For the biodistribution study, a total of 12 nude mice bearing the k562 xenografts were assigned to receive a single 1.0 mg/kg dose intravenous of Q39, and the tumor and organs (kidneys, liver, heart, lung, spleen, brain) were collected at four time points (30, 90, 180, 360 min) after drug administration (n = 3 per time points).

4.3. Drug formulation

Q39 was supplied at a concentration of 1.0 mg/mL in a solution consisting of 0.9% sodium chloride. For all studies requiring lower concentrations of Q39, the stock solution was diluted with 0.9% sodium chloride. Q39 was administered intravenously (i.v.) at a constant concentration of 0.1 mg/mL.

4.4. Toxicology study

ICR mice, 30 males and 30 females, with body weights of 20–24 g, were weighed and observed at least once daily. Six different doses, i.e., 168, 198, 233, 275, 323 and 380 mg/kg of Q39 (formulated in 0.9% sodium chloride) were administered on a single basis intravenously. Each group consisted of ten mice. Clinical signs of toxicity (mortality, activity loss, astasia, hyperspasmia, and loss of body weight), were consecutively observed for 14 days after administration and the half lethal dose (LD_{50}) of intravenous injection in mice was determined following established procedures. Toxicities observed during the course of the study were scored according to their severities using the rating scale described by Patel et al. (2007). Five physical parameters were scored on a scale of 0-4 as follows:(1) mortality: >50% = 4, 50% − 31% = 3, 30% − 11% = 2, 10%–1% = 1, <1% = 0; (2) activity loss: very severe = 4, severe = 3, moderate = 2, slight = 1, none = 0; (3) astasia: very severe = 4, severe = 3, moderate = 2, slight = 1, none = 0; (4) hyperspasmia: very severe = 4, severe = 3, moderate = 2, slight = 1, none = 0; (5) Weight loss: > 10 g = 4, 7–9 g = 3, 4–6 g = 2, 1–3 g = 1, <1 g = 0. The total score for each animal was obtained by adding the five individual scores. Scores are ranked as none (score = 0), mild (score = 1–3), moderate (4–6), and severe (7+).

4.5. Plasma pharmacokinetic and biodistribution study

To characterize the PK of Q39, nude mice bearing the k562 xenografts were bled by cardiac puncture, following a single iv administration at dose levels of 1.0 mg/kg, at the time points of 0.00, 0.17, 0.25, 0.50, 0.75, 1, 1.50, 2, 2.50, 3.00, 4.00, 5.00 and 12 h. At least three animals were used per time point. The blood samples were collected in heparinized tubes by cardiac puncture, and immediately centrifuged at 1500 g for 10 min at 4 °C. Biodistribution studies were carried out until the tumors reached a predetermined target size which was determined by measurement of tumors with a caliper twice a week. To determine tissue distribution, a total of 12 nude mice bearing the k562 xenografts were assigned to receive a single 1.0 mg/kg dose intravenous of Q39. At 30, 90, 180 and 360 min after intravenously administration, mice were sacrificed by cervical dislocation and the tumor and organs (kidneys, liver, heart, lung, spleen, brain) were carefully excised, rinsed with saline and blotted dry. At least three animals were used per time point.

Although Q39 appeared to be relatively stable to light, precautions were taken to minimize exposure to any light source and to the atmosphere. Thus, all samples were protected from light and the plasma was stored at −20 °C without significant decomposition until analysis for Q39.

4.6. Preparation of samples for RRLC-MS/MS analyses

Extraction of Q39 from plasma, tumor, and organ was carried out as described previously (Thomas et al. 2008; Zamboni et al. 2008). To remove surface blood, tissue samples (tumor, organs) were rinsed in physiological saline, blotted dry and weighted. They were then homogenized under an iced bath with 10 times physiological saline (v/w) in a Glas-Col homogenizer system (Glas-Col, Terre Haute, IN). All samples were spiked with gliclazide (IS). Then, for all types of samples, extraction involved solvent precipitation using methanol combined with dimethyl sulfoxide (5:0.1, v/v). Samples were then vortexed, homogenized for 30 min. Tissue and cellular debris were removed by centrifugation (3500 g;15 min). The organic phase was then transferred to a glass tube and evaporated at room temperature for 3 h using a Speedvac apparatus (Savant, USA). The dried sample was reconstituted in 100 µl mobile phase for RRLC-MS/MS analysis. The blank blood and tissue samples obtained from nude mouse were also prepared following the procedure described above.

Stock solutions of 1.0 mg/mL Q39 and 1.0 mg/mL gliclazide (IS) as an internal standard of extraction were prepared in methanol. The 1.0 mg/mL Q39 stock solution for the standard curve and quality control samples were separately prepared. Working standard solutions of Q39 and gliclazide were prepared by appropriate dilutions of the stock solutions in methanol. For preparation of the standards used for construction of calibration curve, 10 µl of working standard solution of Q39 (250, 500, 1000, 2000, 5000, 10 000, 20 000 ng/mL) was added to 90 µl of blank nude mouse plasma or blank tissue samples followed by 1 min vortex. The calibration samples for Q39 are 25, 50, 100, 200, 500, 1 000, 2 000 ng/mL (final concentration). Quality control samples were prepared by adding 10 µl of working standard solution of Q39 (300, 3000 and 15000 ng/mL) to 90 µl of blank nude mouse plasma or blank tissue samples and vortex 1 min. The final concentration of the quality control samples was 30 ng/mL for low quality control (LQC), 300 ng/mL for medium quality control (MQC) and 1500 ng/mL for high quality control (HQC).

4.7. Analytical method for determining Q39 in plasma and tissues

The HPLC system (Agilent RRLC 1200, Agilent Inc, MA, USA) consisted of a quaternary pump, an autosampler, a degasser, an automatic thermostatic column compartment and a computer with Chemstation software (Analyst 1.4.2, Applied Biosystems Inc, USA). The analytical column used was a Zorbax Extend C18 analytical column (3.0 mm × 150 mm, 3.5 µm, Agilent Corporation, MA, USA) with the column temperature set at 20 °C. The mobile phase consisted of methanol–water (75:25, v/v, containing 5 mM ammonia formate), and degassed automatically using the electronic degasser system. The column was equilibrated and eluted under isocratic conditions utilizing a flow rate of 0.3 mL/min. Agilent Technologies 6410 Triple Quad LC/MS equipped with electrospray ionization (ESI) was run by Agilent MassHunter Workstation B.01.03., which was connected to the liquid chromatography system. High-purity nitrogen was provided by a liquid nitrogen tank. The conditions for mass spectrometry were set in the positive selective ion monitoring (SIM) mode using target fragment ions m/z 423.0 for Q39 and m/z 324.0 for the IS. The nebulizer gas pressure was 30 psi with a source temperature of 105 °C. Desolvation gas (nitrogen) was heated to 350 °C and delivered at a flow rate of 8 L/min. The spray voltage was set at 4500 V and collision-induced dissociation (CID) studies were performed with a collision energy of 45 V. The fragmentation energies of Q1 for the analytes were set at 120 V. The optimized collision energies of 20 and 10 eV were used for Q39 and IS, respectively. The ion-spray interface and mass spectrometric conditions were optimized to achieve maximum sensitivity at unit resolution.

The analytical method was validated with respect to linearity, accuracy, precision, recovery and stability. The analytical curves were constructed using seven non-zero standards ranging from 25 to 2000 ng/mL and prepared in eight samples (plasma, tumor, kidneys, liver, heart, lung, spleen, brain). The linearity of the relationship between the peak area ratio and the concentration was demonstrated by the correlation coefficients (r^2) obtained for the linear regression which were >0.999. In order to determine the extraction recovery, another calibration curve was constructed with Q39 methanol solution at a range of 25–2000 ng/mL, after which, known amounts (30, 300 and 1500 ng) of Q39 were added to blank plasma or blank tissue homogenate. The mixtures were analysed by the method described above without IS and the new calibration curve was used to obtain calculated amounts of Q39, with a relative standard deviation (RSD) of <10%. The intra-day and inter-day assay of the method were evaluated by quintuplicate analyses of three quality control samples. The calibration standards and quality controls were analysed on five different days in order to determine intra-day and inter-day precision and accuracy. The accepted criteria for each quality control were that the RSD and accuracy should not exceed 15%.

Three QC samples were determined before and after three freeze-thaw cycles to evaluate the freeze-thaw stability. To evaluate the long-term stability, a long time period (20 days) was defined as the time elapsed between the start of sampling and the end of sample analysis. Aliquots of each sample type were initially frozen at −20 °C and then thawed to be extracted and tested. The difference between the starting concentration and the concentration after 20 days will show whether the drug in plasma can be degraded under these conditions. The results suggest that Q39 is stable at −20 °C.

4.8. Statistical analysis

Pharmacokinetic parameter calculations were carried out using the DAS 2.0 pharmacokinetic program (Chinese Pharmacology Society, Beijing, China). An appropriate pharmacokinetic model was chosen on the lowest Akaike's information criterion (AIC) value (Kieschnick et al. 2003). Maximum plasma concentration (C_{max}) and the time to reach C_{max} (T_{max}) were estimated directly from the observed profiles of plasma level of concentration versus time. The terminal half-life ($T_{1/2}$) was calculated as $0.693/K_{iv}$, and K_{iv} was the slope of the terminal regression line. The area under the curve (AUC) of plasma concentration *vs.* time curve up to the last quantifiable time point, $AUC_{0\text{-}t}$ was obtained by the linear trapezoidal method. The $AUC_{0\text{-}\infty}$ values were calculated to infinity from the model prediction (Kieschnick et al. 2003). The pharmacokinetic parameters, including $AUC_{0\text{-}\infty}$, *CL*, and V_d, were calculated by as the following equations:

$$AUC_{0-\infty} = AUC_{0-t} + C_{last}/K_{iv} \quad (1)$$

$$CL = \frac{D_{iv} \times F_{iv}}{AUC_{0-\infty}} \quad (2)$$

$$V_d = \frac{D_{iv} \times F_{iv}}{C_{in}} \quad (3)$$

where C_{last} is the concentration of the last sampling, D_{iv} is the dose of the compound, F_{iv} is the fraction of dose absorbed, C_{in} represents the estimated initial plasma concentration by extrapolating drug concentration to time zero after iv bolus administration, and Mean residence time (MRT) was determined by division of AUMC (area under the first moment curve) by $AUC_{0\text{-}\infty}$.

The percent of injected dose that localized in per gram tissues or plasma (ID%) and the tumor/nontumor (T/NT) localization ratios were calculated. The results of tissue penetration were calculated by the equation:

$$C_t = \frac{C_S \times V_S}{P_t} \quad (4)$$

$$ID\% = \frac{C_t}{D_{iv}} \times 100\% \quad (5)$$

$$T/NT = \frac{ID\%_{tumor}}{ID\%_{nontumor}} \times 100\% \quad (6)$$

where C_t is the tissue concentration (mg/g), C_s is the supernatant concentration, V_s is the supernatant volume, P_t is the weight of the tissue sample, D_{iv} is the dosage of the compound.

Acknowledgements: This study was supported by grants from the National Post-doctor Foundation of China (NO. 20090460104), the opening foundation of the State Key Laboratory for Diagnosis and Treatment of Infectious Diseases, The First Affiliated Hospital of Medical College, Zhejiang University (No. 2007ZZ10) and Department of Education of Zhejiang Province (NO. 20070076 and Y200909536).

References

Ahlskog JK, Schliemann C, Marlind J, Qureshi U, Ammar A, Pedley RB, Neri D (2009) Human monoclonal antibodies targeting carbonic anhydrase IX for the molecular imaging of hypoxic regions in solid tumours. Br J Cancer 101: 645–657.

Aquino VM, Weitman SD, Winick NJ, Blaney S, Furman WL, Kepner JL, Bonate P, Krailo M, Qu W, Bernstein M (2004) Phase I trial of tirapazamine and cyclophosphamide in children with refractory solid tumors: a pediatric oncology group study. J Clin Oncol 22: 1413–1419.

Chavanpatil MD, Rajeshkumar NV, Gulati A (2006) Determination of endothelin antagonist BMS182874 in plasma by high-performance liquid chromatography. Pharmazie 61: 525–527.

Dorie MJ, Brown JM (1997) Modification of the antitumor activity of chemotherapeutic drugs by the hypoxic cytotoxic agent tirapazamine.Cancer Chemother Pharmacol 39: 361–366.

Fang L, He Q, Hu Y, Yang B (2007) MZ3 induces apoptosis in human leukemia cells. Cancer Chemother Pharmacol 59: 397–405.

Hicks KO, Myint H, Patterson AV, Pruijn FB, Siim BG, Patel K, Wilson WR (2007) Oxygen dependence and extravascular transport of hypoxia-activated prodrugs: comparison of the dinitrobenzamide mustard PR-104A and tirapazamine. Int J Radiat Oncol Biol Phys 69: 560–571.

Graham MA, Senan S, Robin H Jr, Eckhardt N, Lendrem D, Hincks J, Greenslade D, Rampling R, Kaye SB, von Roemeling R, Workman P (1997) Pharmacokinetics of the hypoxic cell cytotoxic agent tirapazamine and its major bioreductive metabolites in mice and humans:retrospective analysis of a pharmacokinetically guided dose-escalation strategy in a phase I trial. Cancer Chemother Pharmacol 40: 1–10.

Hay MP, Hicks KO, Pruijn FB, Pchalek K, Siim BG, Wilson WR, Denny WA (2007) Pharmacokinetic/pharmacodynamic model-guided identification of hypoxia-selective 1,2,4-benzotriazine 1,4-dioxides with antitumor activity: the role of extravascular transport. J Med Chem 50: 6392–6404.

Jiang F, Weng Q, Sheng R, Xia Q, He Q, Yang B, Hu Y. (2007) Synthesis, Structure and Hypoxic Cytotoxicity of 3-Amino-1,2,4-benzotriazine-1,4-dioxide Derivatives. Arch Pharm 340:258–263.

Kieschnick R, McCullough BD (2003) Regression analysis of variates observed on (0, 1): percentages, proportions and fractions. Stat Model 3: 193–213.

Marcu L, Olver I (2006) Tirapazamine: from bench to clinical trials. Curr Clin Pharmacol 1: 71–79.

Patel JB, Khandelwal A, Chopra P, Handratta VD, Njar VC (2007) Murine toxicology and pharmacokinetics of novel retinoic acid metabolism blocking agents. Cancer Chemother Pharmacol 60: 899–905.

Reddy SB, Williamson SK (2009) Tirapazamine: a novel agent targeting hypoxic tumor cells. Expert Opin Investig Drugs 18: 77–87.

Reid JM, Squillace DP, Ames MM (2003) Single-dose pharmacokinetics of the DNA-binding bioreductive agent NLCQ-1 (NSC 709257) in CD2F1 mice. Cancer Chemother Pharmacol 51: 483–487.

Robin HJ, Senan S, Workman P, Graham MA (1995) Development and validation of a sensitive solid-phase-extraction and high-performance liquid chromatography assay for the bioreductive agent tirapazamine and its major metabolites in mouse and human plasma for pharmacokinetically guided dose escalation. Cancer Chemother Pharmacol 36: 266–270.

Rockwell S, Dobrucki IT, Kim EY, Marrison ST, Vu VT (2009) Hypoxia and radiation therapy: past history, ongoing research, and future promise. Curr Mol Med 9: 442–458.

Selvendiran K, Bratasz A, Kuppusamy ML, Tazi MF, Rivera BK, Kuppusamy P (2009) Hypoxia induces chemoresistance in ovarian cancer cells by activation of signal transducer and activator of transcription 3. Int J Cancer 125: 2198–2204.

Steward WP, Middleton M, Benghiat A, Loadman PM, Hayward C, Waller S, Ford S, Halbert G, Patterson LH, Talbot D (2007) The use of pharmacokinetic and pharmacodynamic end points to determine the dose of AQ4N, a novel hypoxic cell cytotoxin, given with fractionated radiotherapy in a phase I study. Ann Oncol 18: 1098–1103.

Svensson KJ, Welch JE, Kucharzewska P, Bengtson P, Bjurberg M, Pahlman S, Ten Dam GB, Persson L, Belting M (2008) Hypoxia-mediated induction of the polyamine system provides opportunities for tumor growth inhibition by combined targeting of vascular endothelial growth factor and ornithine decarboxylase. Cancer Res 68: 9291–9301.

Thomas N, Tirand L, Chatelut E, Plenat F, Frochot C, Dodeller M, Guillemin F, Barberi-Heyob M (2008) Tissue distribution and pharmacokinetics of an ATWLPPR-conjugated chlorin-type photosensitizer targeting neuropilin-1 in glioma-bearing nude mice. Photochem Photobiol Sci 7: 433–441.

Tredan O, Garbens AB, Lalani AS, Tannock IF (2009) The hypoxia-activated prodrug AQ4N penetrates deeply in tumor tissues and complements the limited distribution of mitoxantrone. Cancer Res 69: 940–947.

Weng QJ, Wang DD, Guo P, Fang L, Hu YZ, He QJ, Yang B (2007) Q39, a novel synthetic Quinoxaline 1,4-Di-N-oxide compound with anti-cancer activity in hypoxia. Eur J Pharmacol 581: 262–269.

Yang Bo, Keshelava N, Anderson CP, Reynolds CP (2003) Antagonism of buthionine sulfoximine cytotoxicity for human neuroblastoma cell lines by hypoxia is reversed by the bioreductive agent tirapazamine. Cancer Res 63: 1520–1526.

Yang B, Reynolds CP (2005) Tirapazamine cytotoxicity for neuroblastoma is p53 dependent. Clin Cancer Res 11: 2774–2780.

Zamboni WC, Strychor S, Joseph E, Parise RA, Egorin MJ, Eiseman JL (2008) Tumor, tissue, and plasma pharmacokinetic studies and antitumor response studies of docetaxel in combination with 9-nitrocamptothecin in mice bearing SKOV-3 human ovarian xenografts. Cancer Chemother Pharmacol 62: 417–426.

Zhang B, Weng QJ, Chen ZT (2007) Q39 induces apoptosis in human leukemia cell line K562 in hypoxia. Zhejiang Da Xue Xue Bao Yi Xue Ban 36: 261–266.

Zhu H, Ye L, Richard A, Golbraikh A, Wright FA, Rusyn I, Tropsha A (2009) A novel two-step hierarchical quantitative structure-activity relationship modeling work flow for predicting acute toxicity of chemicals in rodents. Environ Health Perspect 117: 1257–1264.